A framework for feedback stabilization of incompressible flows using quadratic constraints

Talha Mushtaq*
Aerospace Engineering and Mechanics, University of Minnesota, Minneapolis, MN 55455, USA

Peter Seiler†
Electrical Engineering and Computer Science, University of Michigan, Ann Arbor, MI 48109, USA

Maziar S. Hemati,‡
Aerospace Engineering and Mechanics, University of Minnesota, Minneapolis, MN 55455, USA

Flow instabilities can be detrimental for engineered systems interacting with fluids, e.g., through increased drag, vibrations, or heating. Conventional feedback control approaches for stabilizing and suppressing these instabilities rely on linearized models of the fluid dynamics. As such, the resulting controllers tend to suppress instabilities over a narrow range of perturbation magnitudes. In this work, we propose a framework for synthesizing globally stabilizing feedback controllers that can stabilize the flow regardless of the perturbation magnitude. This is done using quadratic constraints that describe input-output properties of the nonlinear terms in the fluid dynamics. In particular, for incompressible flows, the nonlinearity is known to be lossless and energy conserving. The associated quadratic constraint can be used to yield a linear matrix inequality (LMI) for full-state feedback and static output-feedback controller synthesis. We demonstrate that controllers designed by this approach successfully stabilize a reduced-order model of plane Couette flow. We further show that the proposed controllers outperform controllers designed using prevailing linear control synthesis techniques on the same flow.

I. Introduction

Laminar-to-turbulent transition can be undesirable in many engineering systems. Turbulent flows exhibit higher skin-friction drag and heating than laminar flows. Further, fluid-structure interactions involving turbulent flows can deteriorate the health of engineering systems. All of these factors contribute to complications in system design and maintenance needed to contend with wear from high-shear, heating, and vibrations.

Flow control strategies can be employed to suppress laminar-to-turbulent transition. An ability to do this successfully can have economic and performance benefits. One promising approach to flow control is feedback control [1–8]. However, guaranteeing the efficacy of feedback control is difficult due to the nonlinear nature of the fluid dynamics. Feedback controllers are generally designed based on the linearization of nonlinear dynamics about a baseflow [3, 9]. Still, linear design can be challenging because of the non-normal nature of the linearized Navier-Stokes equations [10, 11]. Non-normality of the linear dynamics renders the standard eigenvalue analysis to be less significant in assessing the stability of the system: the linear dynamics can potentially initiate a transient growth in energy despite asymptotic stability [9, 12] .

Despite targeting the relevant linear physics underlying the transition process, linear control practices overlook the significance of nonlinear interactions: controller design relies solely on linear approximations. Indeed, linear control solutions have no a priori guarantees on a controller's stabilization capabilities when subjected to nonlinear flow interactions. A stabilizing linear controller, obtained from linear design methods, will generally only stabilize the nonlinear fluid system over a limited range of perturbation magnitudes [4]: global stability—an important factor to guarantee stabilization in the face of any perturbation magnitude—is not ensured. In such scenarios, an iterative design approach is possible: the user can first design a controller, then proceed to assess its performance after the fact by

---

*Graduate Student, Aerospace Engineering and Mechanics.
†Associate Professor, Electrical Engineering and Computer Science, AIAA Member.
‡Associate Professor, Aerospace Engineering and Mechanics, AIAA Associate Fellow.

either using a campaign of direct numerical simulations (DNS) [4, 5] or recently proposed simulation-free stability analysis techniques [13–15]. The iteration ends when a satisfactory performance objective is reached; otherwise, the objective function is "tuned" in the linear control design method and the process is repeated until a satisfactory solution is obtained. Of course, this iterative design process can be laborious and one will not necessarily know whether or not improved performance can even be achieved. Such complications arise because the overarching control design approach does not directly exploit the knowledge of the nonlinear fluid dynamics.

Our goal here will be to exploit known properties of the nonlinear fluid dynamics to synthesize turbulence-suppressing controllers with guaranteed global stabilization properties. In recent years, several methods exploiting the input-output properties of the quadratic nonlinearity in the nonlinear fluid dynamics have been introduced to analyze global stability for incompressible flows [1, 8, 14, 15]. Several recent studies have developed analysis methods using a quadratic constraint (QC) approach to bound the nonlinear dynamics, enabling estimates on the region of attraction and permissible perturbation thresholds [14–16]. These studies generalize the input-output notion of passivity leveraged in [1, 8].

In this paper, we extend the global stability analysis techniques introduced in [13, 14] to address the control synthesis problem. In particular, we exploit QCs to capture input-output properties of the quadratic (convective) nonlinearity in the fluid dynamics. The resulting control solutions from our QC-based method are globally stabilizing: i.e., the control law robustly stabilizes the flow regardless of the perturbation magnitude. Furthermore, we establish conditions under which such a globally stabilizing controller is feasible. Additionally, we formulate our approach for robustness to parametric variations. Particularly, the synthesis problem yields a single control law that is guaranteed to stabilize the dynamics over a range of Reynolds numbers. The control synthesis is demonstrated on a reduced-order nonlinear model of plane Couette flow [17], which we modify to allow for control action via an artificial modal forcing. The original uncontrolled model has been used previously to demonstrate the potential for nonlinear systems analysis techniques to predict transition [16, 18].

The paper is organized as follows. Section II contains the derivation of the Quadratic Constraint approach and controller synthesis conditions are established at the end of the section. Section III contains a brief description of the reduced-order plane Couette flow model and the results for control design, which are followed by discussion on the effect of critical Reynolds number for flow control. Lastly, Section IV contains the conclusion and future work.

II. Formulation of the Quadratic Constraints

Consider a fluid system with the following state-space form:

$$\begin{aligned}
\dot{\mathbf{x}} &= \mathbf{A}(Re)\mathbf{x} + \mathbf{B}\mathbf{u} + \mathbf{z} \\
\mathbf{z} &= \mathbf{N}(\mathbf{x})\mathbf{x} \\
\mathbf{y} &= \mathbf{C}\mathbf{x}
\end{aligned} \tag{1}$$

where $\mathbf{x} \in \mathbb{R}^n$, $\mathbf{y} \in \mathbb{R}^r$ and $\mathbf{u} \in \mathbb{R}^q$ are state, output and control input vectors, respectively. $\mathbf{A}(Re) \in \mathbb{R}^{n \times n}$ is a linear non-normal system matrix that depends on Reynolds number Re and is asymptotically stable for all Re. $\mathbf{B} \in \mathbb{R}^{n \times q}$ and $\mathbf{C} \in \mathbb{R}^{r \times n}$ are the control input and measurement output matrices, respectively. $\mathbf{N}(\mathbf{x}) : \mathbb{R}^n \to \mathbb{R}^{n \times n}$ is a linear function of $\mathbf{x}$ so that each entry of $\mathbf{z} = \mathbf{N}(\mathbf{x})\mathbf{x}$ is a quadratic function of $\mathbf{x}$. The nonlinearity $\mathbf{z}$ is lossless i.e. $\mathbf{x}^T \mathbf{z} = 0$ for every point in time. This lossless property represents the global behavior of the nonlinearity of the incompressible Navier-Stokes. The nonlinearity is known to redistribute the energy of the fluid system between its velocity modes without creating any energy of its own i.e it is static and lossless, which is common of various shear flows [19]. Therefore, we can make use of this lossless property to bound the nonlinear dynamics of the system to capture its global behavior. Since the nonlinearity is static and lossless, we can perform a Lur'e decomposition of the system as shown in Figure 1. The decomposition indicates a feedback interconnection between the nonlinear and linear dynamics, which is representative of the energy distributive property of the nonlinearity [20].

We assume a control law of the form $\mathbf{u} = \mathbf{K}\mathbf{y}$ for controller design, which results in the closed-loop matrix $\mathbf{A}_{cl}(Re) = \mathbf{A}(Re) + \mathbf{B}\mathbf{K}\mathbf{C}$, where $\mathbf{K} \in \mathbb{R}^{q \times r}$ is a static output-feedback controller gain. Hence, equation (1) can be written as the following:

$$\begin{aligned}
\dot{\mathbf{x}} &= (\mathbf{A}(Re) + \mathbf{B}\mathbf{K}\mathbf{C})\mathbf{x} + \mathbf{z} \\
\mathbf{z} &= \mathbf{N}(\mathbf{x})\mathbf{x} \\
\mathbf{y} &= \mathbf{C}\mathbf{x}.
\end{aligned} \tag{2}$$

Following the work in [14], we use the Lyapunov stability theorem to derive a quadratic constraint with the lossless condition for (2). We start with a candidate Lyapunov function and its time derivative, respectively:
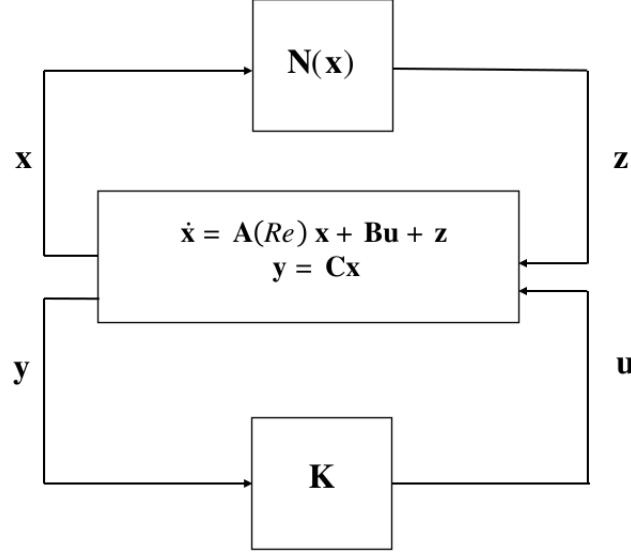
Fig. 1   Lur'e Decomposition of the controlled system

$$V(\mathbf{x}) = \mathbf{x}^T \mathbf{P} \mathbf{x}$$
$$\dot{V}(\mathbf{x}) = 2\mathbf{x}^T \mathbf{P} \dot{\mathbf{x}}.$$

Substituting the dynamics from (2) into $\dot{V}(\mathbf{x})$ yields:

$$\dot{V}(\mathbf{x}) = 2\mathbf{x}^T \mathbf{P}((\mathbf{A}\,(Re) + \mathbf{BKC})\,\mathbf{x} + \mathbf{z}). \tag{3}$$

We can write out $\dot{V}(\mathbf{x})$ into a quadratic form as:

$$\dot{V}(\mathbf{x}) = \begin{bmatrix} \mathbf{x} \\ \mathbf{z} \end{bmatrix}^T \begin{bmatrix} (\mathbf{A}\,(Re) + \mathbf{BKC})^T\,\mathbf{P} + \mathbf{P}\,(\mathbf{A}\,(Re) + \mathbf{BKC}) & \mathbf{P} \\ \mathbf{P} & \mathbf{0} \end{bmatrix} \begin{bmatrix} \mathbf{x} \\ \mathbf{z} \end{bmatrix}.$$

The global stability condition to satisfy is $\dot{V}(\mathbf{x}) \leq -\epsilon V(\mathbf{x})$, where $\epsilon > 0$. We introduce a Lagrange multiplier ξ_0 for the lossless property $\mathbf{x}^T \mathbf{z} = 0$ such that $\dot{V}(\mathbf{x}) + 2\xi_0 \mathbf{x}^T \mathbf{z} \leq -\epsilon V(\mathbf{x})$ [14]. This can be written as:

$$\begin{bmatrix} \mathbf{x} \\ \mathbf{z} \end{bmatrix}^T \left\{ \begin{bmatrix} (\mathbf{A}\,(Re) + \mathbf{BKC})^T\,\mathbf{P} + \mathbf{P}\,(\mathbf{A}\,(Re) + \mathbf{BKC}) & \mathbf{P} \\ \mathbf{P} & \mathbf{0} \end{bmatrix} + \xi_0 \begin{bmatrix} \mathbf{0} & \mathbf{I} \\ \mathbf{I} & \mathbf{0} \end{bmatrix} + \begin{bmatrix} \epsilon\mathbf{P} & \mathbf{0} \\ \mathbf{0} & \mathbf{0} \end{bmatrix} \right\} \begin{bmatrix} \mathbf{x} \\ \mathbf{z} \end{bmatrix} \leq 0. \tag{4}$$

Thus, we can obtain a globally stabilizing controller $\mathbf{K}$ by solving the following for a fixed Re:

$$\begin{bmatrix} (\mathbf{A}\,(Re) + \mathbf{BKC})^T\,\mathbf{P} + \mathbf{P}\,(\mathbf{A}\,(Re) + \mathbf{BKC}) & \mathbf{P} \\ \mathbf{P} & \mathbf{0} \end{bmatrix} + \xi_0 \begin{bmatrix} \mathbf{0} & \mathbf{I} \\ \mathbf{I} & \mathbf{0} \end{bmatrix} + \begin{bmatrix} \epsilon\mathbf{P} & \mathbf{0} \\ \mathbf{0} & \mathbf{0} \end{bmatrix} \leq 0 \tag{5}$$

$$\mathbf{P} > 0.$$

For fluid systems, a globally stabilizing controller implies that the system will have a monotonic decay in Transient Energy growth (TEG), which is defined as [3]:

$$\mathcal{E}(t) = \frac{E(t)}{E(0)} = \frac{\mathbf{x}(t)^T \mathcal{W} \mathbf{x}(t)}{\mathbf{x}(0)^T \mathcal{W} \mathbf{x}(0)} \tag{6}$$

where $\mathcal{W}$ is the weight matrix and $\mathbf{x}(0)$ is the initial state vector. The transient growth phenomenon is an inherent characteristic of fluid systems, where despite the asymptotically stable matrix $\mathbf{A}(Re)$, the system can be destabilized. Specifically, the transient growth is the direct consequence of the non-normality of the matrix $\mathbf{A}(Re)$ [12]. However, the global behavior of the system is dependent on the interactions between the linear and nonlinear terms, which can lead to an onset of flow transition to turbulence [14]. Therefore, our approach directly constrains the lossless behaviour of the nonlinear interactions to achieve global stability.

3

Notice that the matrix inequality in (5) is bilinear in variables $\mathbf{P}$ and $\mathbf{K}$. However, one can see that for the inequality in (5) to be satisfied, the off-diagonal terms must cancel i.e. $\mathbf{P} = -\xi_0\mathbf{I}$. Since ξ_0 is a scalar variable, we can scale it to be $\xi_0 = -1$ because $\mathbf{P} > 0$. Therefore, we only need to satisfy the following Linear Matrix Inequality (LMI) to obtain a globally stabilizing controller for a given Re:

$$(\mathbf{A}\,(Re) + \mathbf{BKC})^T + \mathbf{A}\,(Re) + \mathbf{BKC} + \epsilon\mathbf{I} \le 0. \tag{7}$$

Notice that (7) is convex for state-feedback and static output-feedback (SOF) controllers. We will design each controller for a fixed Re, which we will denote as Re_{syn}. The controller obtained using the LMI in (7) is globally stablizing for all $Re \le Re_{syn}$ [13]. The LMIs formulated in this paper are only valid for the models that are in a co-ordinate system, where the energy of the system can be represented as identity. We use (7) to design controllers for a reduced-order plane Couette flow model* following the work in [13].

III. Results

In this section, we will demonstrate the application of the QC framework on the 9-state reduced-order model of a plane Couette flow *. This 9-state model is an improved model for sustained turbulence, which was first introduced by [17]. The model has been used as a benchmark for new analysis methods, such as in [18] where global stability analysis was studied using sum-of-squares (SOS) optimization techniques. Low-order basis functions * were used to formulate a state-space description of the system similar to (1), but without the control input $\mathbf{u}$. In this work, we augment the reduced-order model with a control input to model actuation. This is done through an artificial modal forcing that acts directly on a subset of the model states. Specific details will be given in the next section.

All the controller analysis in this paper is done using an optimal disturbance that drives the nonlinear dynamics of the controlled or uncontrolled system toward instability. These optimal disturbances maximize the transient energy growth in the nonlinear system for a disturbance with a given magnitude, and are computed using direct-adjoint looping methods [21]. We compare our controllers against a state-feedback Linear Quadratic Regulator (LQR) as it is a commonly used benchmark technique for flow control. We simulate the designed controllers to study the transient growth of the system defined in (6) to assess the global stability of the controlled system. Weighting matrix $\mathcal{W} = \mathbf{I}$ for all calculations, where $\mathbf{I} \in \mathbb{R}^{n\times n}$ is identity.

It is well-known that fluid flows exhibit transient energy growth (TEG) beyond their critical Reynolds number Re_{cr}, which can result in flow instabilities. For a given $Re > Re_{cr}$, these instabilities are triggered by an increase in TEG beyond a certain energy threshold, which can result in flow transition to turbulence. However, by ensuring that we have unit TEG, i.e., $\{\max_{t\ge 0}\mathcal{E}(t)\} = 1$, we prevent the onset of any flow instabilities because unit TEG is a necessary condition for global stability of incompressible flows. Thus, all controllers are designed for $Re_{syn} > Re_{cr}$ to ensure a unit TEG between Re_{syn} and Re_{cr}, where Re_{syn} is the controller synthesis Reynolds number. The reduced-order plane Couette flow model has $Re_{cr} = 7.9$ for the parameters described in Appendix A. Therefore, we choose $Re_{syn} = 8 > Re_{cr}$. The critical Reynolds number can be calculated by simply solving (5) for $\mathbf{B} = 0$ and $\mathbf{C} = 0$ for various Re until (5) is no longer feasible. In other words, $\mathbf{A}(Re) + \mathbf{A}^T(Re) \not< 0$ for $Re > Re_{cr}$ (see [13]). Additionally, we show that for a given state-feedback or output-feedback controller, the controlled system's critical Reynolds number increases. We will denote the critical Reynolds number associated with the controlled fluid system as $Re_{cr,c}$.

A. Controller Design

In this section, we design and test the controllers at an off-design Re to check for global stability and robustness to Re variations. We study the following three types of controllers: LQR, state-feedback Quadratic Constraint (QC) and static output-feedback Quadratic Constraint (SOF-QC). The LQR controller is determined from minimizing the cost function:

$$\mathbf{J} = \int_0^\infty \mathbf{x}^T\mathbf{Q}\mathbf{x} + \mathbf{u}^T\mathbf{R}\mathbf{u}\ dt \tag{8}$$

where $\mathbf{Q}$ and $\mathbf{R}$ are the state and input weighting matrices, respectively. Since LQR requires a linear dynamical system, we can linearize † the system equation in (2) about the equilibrium vector $\mathbf{x}_{eq} = \mathbf{0}$. The weighting matrices $\mathbf{Q}$ and $\mathbf{R}$ are chosen to be $\mathbf{I}_{9\times 9}$ and $0.1 \times \mathbf{I}_{6\times 6}$, respectively. The state-feedback and static output-feedback controllers are simply
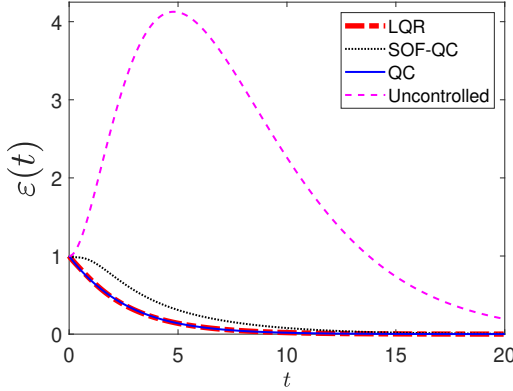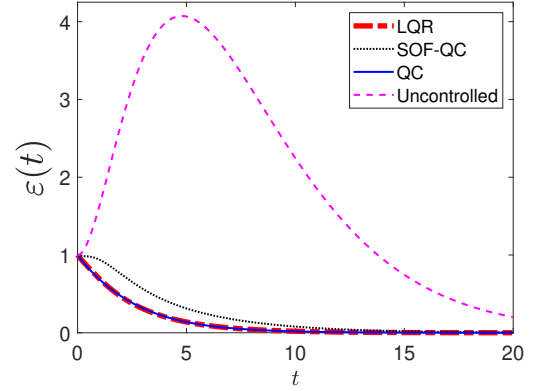
---

* See Appendix A

† See Appendix B

determined from solving (7). The LMI in (7) is solved using *cvx* [22] with MOSEK solver option. We set the input matrix **B** and output matrix **C** as the following for state-feedback and output-feedback controllers:

$$Static - Output\ Feedback : \mathbf{B} = \begin{bmatrix} \mathbf{I}_{6\times6} \\ \mathbf{0}_{3\times6} \end{bmatrix}, \quad \mathbf{C} = \mathbf{B}^T$$

$$State - Feedback : \mathbf{B} = \begin{bmatrix} \mathbf{I}_{6\times6} \\ \mathbf{0}_{3\times6} \end{bmatrix}, \quad \mathbf{C} = \mathbf{I}$$

(9)

where $\mathbf{I}_{6\times6} \in \mathbb{R}^{6\times6}$ is the identity matrix.

(a) $\quad \|x(0)\| = 0.05$ **(b)** $\quad \|x(0)\| = 0.1$

Fig. 2   **The energy plots in (a) and (b) for** $Re = 20$ **indicate that the controller is restricting the energy of the system below** $\mathcal{E}(t) = 1$. **Additionally, increasing** $\|x(0)\| = 0.05 \rightarrow 0.1$ **does not destabilize the controlled system since** $\mathcal{E}(t) \leq 1$ **as** $t \rightarrow \infty$.

Figures 2(a) and (b) show the energy response curves for SOF-QC, QC and LQR controllers. The controllers in figures 2(a) and (b) are designed for $Re_{syn} = 8$ and are tested for $Re = 20$. We observe in figure 2(a) that the controlled system for $Re = 20$ indeed has a monotonically decaying energy for the optimal initial state of magnitude $\|\mathbf{x}(0)\| = 0.05$. Therefore, any initial state of magnitude $\|\mathbf{x}(0)\| \leq 0.05$ will have a monotonic decay in energy. To show that the system is in fact globally stable, we increase $\|\mathbf{x}(0)\|$ to 0.1 for the same controllers. We can see in figure 2(b) that increasing $\|\mathbf{x}(0)\|$ does not affect the energy response of the controlled system as there is a monotonic energy decay, thus, the system is globally stable. In fact $\|\mathbf{x}(0)\|$ can be increased to larger magnitudes such as $\|\mathbf{x}(0)\| = 10$. However, $\|\mathbf{x}(0)\| = 0.1$ is sufficiently large to showcase global stability for this system since the uncontrolled system exhibits transient growth. Furthermore, it can be shown that the controller designed for $Re_{syn} = 8$ is globally stabilizing for the off-design Reynolds number of $Re = 20$ [13]: i.e., monotonic energy decay will be observed for all perturbation magnitudes. On the contrary, the uncontrolled system, as observed in figures 2(a) and (b) has a peak of $\mathcal{E}(t) \approx 4$, therefore, the uncontrolled system is not globally stable. Although the energy eventually decays to zero for the uncontrolled system, there exists a perturbation $\|\mathbf{x}(0)\|$ such that the system will never return to the origin (transition to turbulence) [2, 21]. Also notice that both the state-feedback controllers QC and LQR have similar rate of decay. In figures 2(a) and (b) the growth in TEG is a result of $Re > Re_{cr}$ for the uncontrolled system. Similarly, if we increased Re such that $Re > Re_{cr,c}$ for a fixed $\|\mathbf{x}(0)\|$ then we will also observe an increase in TEG for the controlled system, i.e., $\{\max_{t \geq 0} \mathcal{E}(t)\} > 1$. Thus, the controlled system will no longer be globally stable.

B. Critical Reynolds Number

We see in figure 3 that the SOF-QC controller has a large transient growth for $Re = 600$ and $\|\mathbf{x}(0)\| = 0.1$. These growths occur because $Re = 600$ is much larger than the critical Reynolds number of the controlled system $Re_{cr,c}$ as

seen in Table 1. It has been noted by the authors of [9] that $\mathbf{A}(Re) + \mathbf{A}(Re)^T \nprec 0$ is a necessary and sufficient condition for non-monotonic decay in TEG. If $\mathbf{A}(Re) + \mathbf{A}(Re)^T < 0$ then $\{\max_{t \geq 0} \mathcal{E}(t)\}$ will be unity, which is precisely the condition each controller must satisfy. This condition is violated when $Re > Re_{cr,c}$ for any given controller. Thus, we see an increase in TEG in figure 3. However, this can be remedied by simply designing a controller at a sufficiently high Re_{syn}, which would ensure global stability for any $Re \leq Re_{syn}$. Notice that the global stability condition in (7) is exactly the necessary and sufficient condition described in [9]. The main purpose of computing $Re_{cr,c}$ is to show

Systems	Critical Reynolds Number
Uncontrolled	7.90
Static Output Feedback - QC (SOF-QC)	21.15
State Feedback - LQR (LQR)	151.51
State Feedback - QC (QC)	200,000.00

Table 1   Table shows critical Reynolds numbers for different systems. Critical Reynolds number for the QC controller is the maximum grid size. The actual critical Reynolds number is higher.

that accounting for nonlinear interactions in controller design increases the critical Reynolds number for the controlled fluid flow. The QC controller has identical system and input matrices to the LQR, yet it has a much larger $Re_{cr,c}$. The $Re_{cr,c}$ listed in table 1 for QC controller is the maximum value of $Re_{cr,c}$ search grid. The actual value of $Re_{cr,c}$ is in fact larger. Additionally, the weighting matrix $\mathbf{R}$ for LQR was chosen such that $Re_{cr,c}$ has the largest value for the LQR controller. Since $Re > Re_{cr,c}$ in figure 3 for the LQR controller, we see an approximately 1% transient growth, hence the LQR controller is not globally stabilizing. Therefore, enforcing the global behavior of the nonlinearity allows for better control.
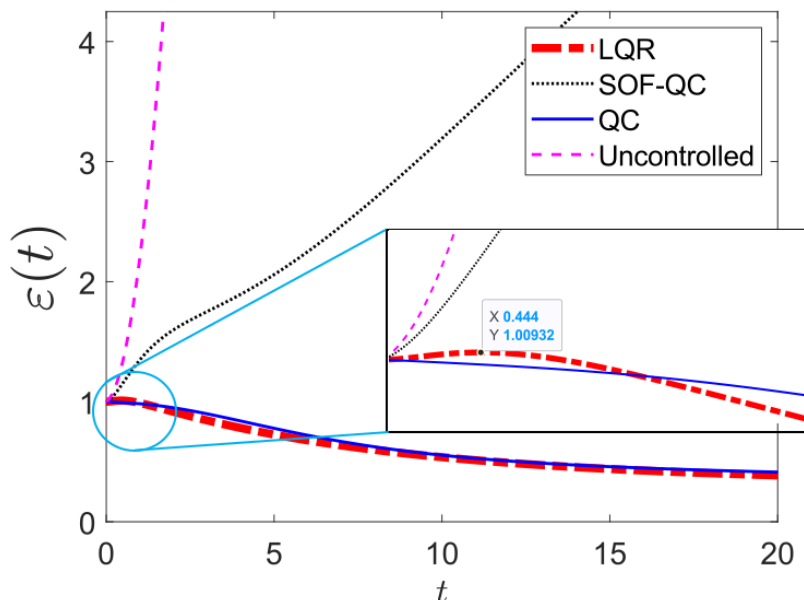

Fig. 3   Energy profile at $\|x(0)\| = 0.1$ and $Re = 600$. The LQR and SOF-QC exhibit transient energy growth and therefore are not globally stable controllers.

IV. Conclusion and Future Work

The synthesis method introduced in this paper allows us to exploit the conservative property of the quadratic nonlinearity of the fluid system. Using the Lyapunov stability condition, we can essentially introduce properties of fluid systems as a set of quadratic constraints. This allows for some flexibility in the method as we can introduce additional quadratic constraints on the system such as the local constraints [14], [15]. The primary drawback of the QC-based

approach is the computational complexity of available solution algorithms. This is not necessarily a limitation provided that low-order descriptions of the fluid dynamics are available. The QC framework can be extended to account for associated model uncertainties in low-order fluids models, and this will be the subject of future work.

External noise and disturbances were ignored for the controller design process in this paper, which are common in realistic systems. Using a set of quadratic constraints to impose exogenous signal constraints is part of future study. Additionally, we plan to introduce tuning parameters to offer more flexibility in the control design. This will include an ability to penalize control effort within the QC-based controller synthesis framework. Although our discussions were limited to state-feedback and output-feedback controllers in this paper, we can design more types of controllers to achieve global stability such as a dynamic output-feedback controller. In general, state-feedback controllers are impractical because perfect state information is never possible. Finally, the controllers that depend on state estimation, such as the Linear Quadratic Gaussian (LQG), have shown to further deteriorate the system performance [3, 11]. A QC-based synthesis framework would provide a means of designing dynamic compensators that are guaranteed to stabilize the fluid dynamics and suppress transition.

V. Acknowledgements

References

[1] Sharma, A., Morrison, F., J, McKeon, B. J., and Limebeer, W., D.J.N. Koberg, "Relaminarisation of $Re_\tau = 100$ channel flow with globally stabilising linear feedback control," *Physics of Fluids*, 2011.

[2] Burns, J. A., and Singler, J., "Feedback control of low dimensional models of transition to turbulence," *Proceedings of the 44th IEEE Conference on Decision and Control*, 2005, pp. 3140–3145.

[3] McKernan, J., "Control of plane Poiseuille flow: a theoretical and computational investigation," Ph.D. thesis, Cranfield University, 2006.

[4] Sun, Y., and Hemati, M. S., "Feedback Control for Transition Suppression in Direct Numerical Simulations of Channel Flow," *Energies*, Vol. 12, No. 21, 2019.

[5] Yao, H., Sun, Y., Mushtaq, T., and Hemati, M. S., "Reducing Transient Energy Growth in a Channel Flow Using Static Output Feedback Control," *AIAA Journal*, Vol. 0, No. 0, 2022, pp. 1–14.

[6] Högberg, M., Bewley, T. R., and Henningson, D. S., "Linear feedback control and estimation of transition in plane channel flow," *Journal of Fluid Mechanics*, Vol. 481, 2003, pp. 149–175.

[7] Bewley, T., and Moin, P., "Optimal control of turbulent channel flows," *Active Control of Vibration and Noise*, Vol. 75, 1994, pp. 221–227.

[8] Heins, P. H., Jones, B. L., and Sharma, A. S., "Passivity-based output-feedback control of turbulent channel flow," *Automatica*, 2016.

[9] Whidborne, J. F., and McKernan, J., "On the minimization of maximum transient energy growth," *IEEE transactions on automatic control*, Vol. 52, No. 9, 2007, pp. 1762–1767.

[10] Schmid, P. J., and Henningson, D. S., *Stability and transition in shear flows*, Springer, 2001.

[11] Hemati, M. S., and Yao, H., "Performance Limitations of Observer-Based Feedback for Transient Energy Growth Suppression," *AIAA Journal*, Vol. 56, No. 6, 2018.

[12] Plischke, E., "Transient effects of linear dynamical systems," Ph.D. thesis, Universität Bremen, 2005.

[13] Mushtaq, T., Seiler, P., and Hemati, M., "Feedback control of transitional flows: A framework for controller verification using quadratic constraints," *AIAA AVIATION 2021 FORUM, AIAA Paper 2021-2825*, 2021, p. 2825.

[14] Kalur, A., Seiler, P., and Hemati, M. S., "Nonlinear stability analysis of transitional flows using quadratic constraints," *Physical Review Fluids*, Vol. 6, No. 4, 2021.

[15] Liu, C., and Gayme, D. F., "Input-output inspired method for permissible perturbation amplitude of transitional wall-bounded shear flows," *Physical Review E*, Vol. 102, No. 6, 2020.

[16] Kalur, A., Mushtaq, T., Seiler, P., and Hemati, M. S., "Estimating regions of attraction for transitional flows using quadratic constraints," *IEEE Control Systems Letters*, Vol. 6, 2021, pp. 482–487.

[17] Moehlis, J., Faisst, H., and Eckhardt, B., "A low-dimensional model for turbulent shear flows," *New Journal of Physics*, Vol. 6, No. 1, 2004, p. 56.

[18] Goulart, P. J., and Chernyshenko, S., "Global stability analysis of fluid flows using sum-of-squares," *Physica D: Nonlinear Phenomena*, Vol. 241, No. 6, 2012, p. 692–704.

[19] Baggett, J. S., and Trefethen, L. N., "Low-dimensional models of subcritical transition to turbulence," *Physics of Fluids*, Vol. 9, No. 4, 1997, pp. 1043–1053.

[20] Khalil, H. K., *Nonlinear systems; 3rd ed.*, Prentice-Hall, 2002.

[21] Kerswell, R., "Nonlinear Nonmodal Stability Theory," *Annual Review of Fluid Mechanics*, Vol. 50, No. 1, 2018, pp. 319–345.

[22] Grant, M., Boyd, S., and Ye, Y., "CVX: Matlab software for disciplined convex programming," , 2008.

Appendix A: Reduced-Order Model of a Transitional Plane Couette Flow

The model is derived from a low-order approximation of a plane Couette flow using the data from direct numerical simulations (DNS) [17]. Low-order basis functions $\mathbf{s}_i$ are used to construct a state-space system:

$$\dot{\mathbf{x}} = \mathbf{A}(Re)\mathbf{x} + \mathbf{z} \tag{10}$$

where,

$\mathbf{A}(Re) = \frac{\mathbf{\Lambda}}{\mathbf{Re}} + \mathbf{W}$

$\mathbf{\Lambda} = -diag\left(\beta^2, \frac{4\beta^2}{3} + \gamma^2, \kappa_{\beta\gamma}^2, \frac{3\alpha^2+4\beta^2}{3}, \kappa_{\alpha\beta}^2, \frac{3\alpha^2+4\beta^2+3\gamma^2}{3}, \kappa_{\alpha\beta\gamma}^2, \kappa_{\alpha\beta\gamma}^2, 9\beta^2\right),$

$\mathbf{W}\mathbf{x} = \mathbf{N}(\mathbf{x})\mathbf{c} + \mathbf{N}(\mathbf{c})\mathbf{x}$

$\mathbf{z} = \mathbf{N}(\mathbf{x})\mathbf{x}.$

The parameters α, β, γ, $\mathbf{c}$, L_x and L_z are chosen as the following: $\alpha = \frac{2\pi}{L_x}$, $\beta = \frac{\pi}{2}$, $\gamma = \frac{2\pi}{L_z}$, $\mathbf{c} = vec(1, 0, ..., 0)$, $L_x = 1.75\pi$ and $L_z = 1.5\pi$, where $vec(..)$ represents a vector of constants. Some notations are defined as the following for the sake of convenience: $\kappa_{\alpha\beta\gamma} = \sqrt{\alpha^2 + \beta^2 + \gamma^2}$, $\kappa_{\beta\gamma} = \sqrt{\beta^2 + \gamma^2}$ and $\kappa_{\alpha\beta} = \sqrt{\alpha^2 + \beta^2}$. Finally, the individual entries in the nonlinearity $\mathbf{z}$ are the following:

$[\mathbf{N}(\mathbf{x})\mathbf{x}]_1 = \sqrt{\frac{3}{2}}\frac{\beta\gamma}{\kappa_{\beta\gamma}}x_2x_3 - \sqrt{\frac{3}{2}}\frac{\beta\gamma}{\kappa_{\alpha\beta\gamma}}x_6x_8$

$[\mathbf{N}(\mathbf{x})\mathbf{x}]_2 = \frac{10}{3\sqrt{6}}\frac{\gamma^2}{\kappa_{\alpha\gamma}}x_4x_6 - \frac{\gamma^2}{\sqrt{6}\kappa_{\alpha\gamma}}x_5x_7 - \frac{\alpha\beta\gamma}{\sqrt{6}\kappa_{\alpha\gamma}\kappa_{\alpha\beta\gamma}}x_5x_8 - \sqrt{\frac{3}{2}}\frac{\beta\gamma}{\kappa_{\beta\gamma}}(x_1x_3 + x_3x_9)$

$[\mathbf{N}(\mathbf{x})\mathbf{x}]_3 = \sqrt{\frac{2}{3}}\frac{\alpha\beta\gamma}{\kappa_{\alpha\gamma}\kappa_{\beta\gamma}}(x_5x_6 + x_4x_7) + \frac{\beta^2(3\alpha^2+\gamma^2)-3\gamma^2\kappa_{\alpha\gamma}^2}{\sqrt{6}\kappa_{\alpha\gamma}\kappa_{\beta\gamma}\kappa_{\alpha\beta\gamma}}$

$[\mathbf{N}(\mathbf{x})\mathbf{x}]_4 = -\frac{\alpha}{\sqrt{6}}(x_1x_5 + x_5x_9) - \frac{10}{3\sqrt{6}}\frac{\alpha^2}{\kappa_{\alpha\gamma}}x_2x_6 - \sqrt{\frac{3}{2}}\frac{\alpha\beta\gamma}{\kappa_{\alpha\gamma}\kappa_{\beta\gamma}}x_3x_7 - \sqrt{\frac{3}{2}}\frac{\alpha^2\beta^2}{\kappa_{\alpha\gamma}\kappa_{\beta\gamma}\kappa_{\alpha\beta\gamma}}x_3x_8$

$[\mathbf{N}(\mathbf{x})\mathbf{x}]_5 = \frac{\alpha}{\sqrt{6}}(x_1x_4 + x_4x_9) + \sqrt{\frac{2}{3}}\frac{\alpha\beta\gamma}{\kappa_{\alpha\gamma}\kappa_{\beta\gamma}}x_3x_6 + \frac{\alpha^2}{\sqrt{6}\kappa_{\alpha\gamma}}x_2x_7 - \frac{\alpha\beta\gamma}{\sqrt{6}\kappa_{\alpha\gamma}\kappa_{\alpha\beta\gamma}}x_2x_8$

$[\mathbf{N}(\mathbf{x})\mathbf{x}]_6 = \frac{10}{3\sqrt{6}}\frac{\alpha^2-\gamma^2}{\kappa_{\alpha\gamma}}x_2x_4 - \sqrt{\frac{2}{3}}\frac{2\alpha\beta\gamma}{\kappa_{\alpha\gamma}\kappa_{\beta\gamma}}x_3x_5 + \frac{\alpha}{\sqrt{6}}(x_1x_7 + x_7x_9) + \sqrt{\frac{3}{2}}\frac{\beta\gamma}{\kappa_{\alpha\beta\gamma}}(x_1x_8 + x_8x_9)$

$[\mathbf{N}(\mathbf{x})\mathbf{x}]_7 = \frac{\alpha\beta\gamma}{\sqrt{6}\kappa_{\alpha\gamma}\kappa_{\beta\gamma}}x_3x_4 + \frac{-\alpha^2+\gamma^2}{\sqrt{6}\kappa_{\alpha\gamma}}x_2x_5 - \frac{\alpha}{\sqrt{6}}(x_1x_6 + x_6x_9)$

8

$$[\mathbf{N}(\mathbf{x})\mathbf{x}]_8 = \frac{\gamma^2(3\alpha^2-\beta^2+3\gamma^2)}{\sqrt{6}\kappa_{\alpha\gamma}\kappa_{\beta\gamma}\kappa_{\alpha\beta\gamma}}x_3x_4 + \sqrt{\frac{2}{3}}\frac{\alpha\beta\gamma}{\kappa_{\alpha\gamma}\kappa_{\alpha\beta\gamma}}x_2x_5$$

$$[\mathbf{N}(\mathbf{x})\mathbf{x}]_9 = \sqrt{\frac{3}{2}}\frac{\beta\gamma}{\kappa_{\beta\gamma}}x_2x_3 - \sqrt{\frac{3}{2}}\frac{\beta\gamma}{\kappa_{\alpha\beta\gamma}}x_6x_8$$

where z_i represents the i-th element of $\mathbf{z}$. The domain sizes L_x and L_z are chosen such that they are greater than the minimal flow unit. A minimal flow unit is considered to be the smallest numerical domain for which we can have numerically sustained turbulence [17]. Similar domain size has been used by the authors in [17] for analysis. Furthermore, the constants in $\mathbf{c}$ are chosen such that the steady flow solution $\bar{\mathbf{s}}$ is spanned by the basis $\mathbf{s}_i$, i.e., $\bar{\mathbf{s}} = \mathbf{s}_i c_i$, where c_i is the i-th element of $\mathbf{c}$. Further in-depth details are given in [17, 18] about the derivation of the nonlinearity and the model. The following are the basis $\mathbf{s}_i$ for the reduced-order model:

The basic profile:

$$1)\ \mathbf{s}_1 = \begin{bmatrix} \sqrt{2}sin(\pi y/2) \\ 0 \\ 0 \end{bmatrix}$$

The streak:

$$2)\ \mathbf{s}_2 = \begin{bmatrix} \frac{4}{\sqrt{3}}cos^2(\pi y/2)cos(\gamma z) \\ 0 \\ 0 \end{bmatrix}$$

The downstream vortex:

$$3)\ \mathbf{s}_3 = \frac{2}{\sqrt{4\gamma^2+\pi^2}} \begin{bmatrix} 0 \\ 2\gamma cos(\pi y/2)cos(\gamma z) \\ \pi sin(\pi y/2)sin(\gamma z) \end{bmatrix}$$

The spanwise flows:

$$4)\ \mathbf{s}_4 = \begin{bmatrix} 0 \\ 0 \\ \frac{4}{\sqrt{3}}cos(\alpha x)cos^2(\pi y/2) \end{bmatrix}$$

$$5)\ \mathbf{s}_5 = \begin{bmatrix} 0 \\ 0 \\ 2sin(\alpha x)sin(\pi y/2) \end{bmatrix}$$

The normal vortex modes:

$$6)\ \mathbf{s}_6 = \frac{4\sqrt{2}}{\sqrt{3(\alpha^2+\gamma^2)}} \begin{bmatrix} -\gamma cos(\alpha x)cos^2(\pi y/2)sin(\gamma z) \\ 0 \\ \alpha sin(\alpha x)cos^2(\pi y/2)cos(\gamma z) \end{bmatrix}$$

$$7)\ \mathbf{s}_7 = \frac{2\sqrt{2}}{\sqrt{\alpha^2+\gamma^2}} \begin{bmatrix} \gamma sin(\alpha x)sin(\pi y/2)sin(\gamma z) \\ 0 \\ \alpha cos(\alpha x)sin(\pi y/2)cos(\gamma z) \end{bmatrix}$$

Three-dimensional mode:

$$8)\ \mathbf{s}_8 = \frac{2\sqrt{2}}{\sqrt{(\alpha^2+\gamma^2)(4\alpha^2+4\gamma^2+\pi^2)}} \begin{bmatrix} \pi sin(\alpha x)sin(\pi y/2)sin(\gamma z) \\ 2(\alpha^2 + \gamma^2)cos(\alpha x)cos(\pi y/2)sin(\gamma z) \\ -\pi cos(\alpha x)sin(\pi y/2)cos(\gamma z) \end{bmatrix}$$

Modification to the basic profile due to turbulence:

$$9) \; \mathbf{s}_9 = \begin{bmatrix} \sqrt{2} sin(3\pi y/2) \\ 0 \\ 0 \end{bmatrix}$$

The normal vortex mode and the three-dimensional mode result from the advection of $\mathbf{s}_4$ and $\mathbf{s}_5$ by the streak mode $\mathbf{s}_2$ and vortex mode $\mathbf{s}_3$.

Appendix B: LQR Design

The LQR controller gain can be found by linearizing our system in (1). We use the MATLAB function *lqr* for solving the Algebraic Riccati Equations. The linearised system has the form:

$$\delta \dot{\mathbf{x}} = \bar{\mathbf{A}} \delta \mathbf{x} + \bar{\mathbf{B}} \delta \mathbf{u}$$

where

$$\bar{\mathbf{A}} = \begin{bmatrix} \frac{\partial f_1(x,u)}{\partial x_1} & \frac{\partial f_1(x,u)}{\partial x_2} & \frac{\partial f_1(x,u)}{\partial x_3} & \cdots & \frac{\partial f_1(x,u)}{\partial x_n} \\ \vdots & \vdots & \vdots & \vdots & \vdots \\ \frac{\partial f_n(x,u)}{\partial x_1} & \frac{\partial f_n(x,u)}{\partial x_2} & \frac{\partial f_n(x,u)}{\partial x_3} & \cdots & \frac{\partial f_n(x,u)}{\partial x_n} \end{bmatrix} \quad (11)$$

$$\bar{\mathbf{B}} = \begin{bmatrix} \frac{\partial f_1(x,u)}{\partial u_1} & \frac{\partial f_1(x,u)}{\partial u_2} & \frac{\partial f_1(x,u)}{\partial u_3} & \cdots & \frac{\partial f_1(x,u)}{\partial u_p} \\ \vdots & \vdots & \vdots & \vdots & \vdots \\ \frac{\partial f_n(x,u)}{\partial u_1} & \frac{\partial f_n(x,u)}{\partial u_2} & \frac{\partial f_n(x,u)}{\partial u_3} & \cdots & \frac{\partial f_n(x,u)}{\partial u_p} \end{bmatrix}$$

where n and p are the number of states and control inputs, respectively. In our system $n = 9$ and $p = 6$. The control law has the form $\delta \mathbf{u} = \mathbf{K}_{lqr} \delta \mathbf{x}$, where $\delta \mathbf{x} = \mathbf{x} - \mathbf{x}_{eq}$ and $\delta \mathbf{u} = \mathbf{u} - \mathbf{u}_{eq}$; $\mathbf{u}_{eq} = \mathbf{0}$ and $\mathbf{x}_{eq} = \mathbf{0}$ are the equilibrium points. Now, the linearised system in (11) can be used to find the LQR gain $\mathbf{K}_{lqr}$. To simulate the full response of the LQR, we will make use of $\bar{A}$ and $\bar{B}$ and then add back the equilibrium solutions, which in this case are just zero. Hence $\delta \mathbf{x} = \mathbf{x}$ and $\delta \mathbf{u} = \mathbf{u}$.